frontiers | Frontiers in Physics

TYPE Original Research
PUBLISHED 04 January 2023
DOI 10.3389/fphy.2022.1038905



OPEN ACCESS

EDITED BY
Farruh Atamurotov,
Inha University in Tashkent, Uzbekistan

REVIEWED BY
Abdul Jawad,
COMSATS University Islamabad, Pakistan
Izzet Sakalli,
Eastern Mediterranean University, Turkey
Ali Övgün,
Eastern Mediterranean University, Turkey

*CORRESPONDENCE
Ksh. Newton Singh,
newton.kshetrimayum@associates.iucaa.in

SPECIALTY SECTION
This article was submitted to Cosmology, a section of the journal Frontiers in Physics

RECEIVED 07 September 2022
ACCEPTED 07 December 2022
PUBLISHED 04 January 2023

CITATION
Singh KN, Rahaman F, Deb D and Maurya SK (2023), Traversable Finslerian wormholes supported by phantom energy.
*Front. Phys.* 10:1038905.
doi: 10.3389/fphy.2022.1038905



# Traversable Finslerian wormholes supported by phantom energy

Ksh. Newton Singh[1]*, Farook Rahaman[2], Debabrata Deb[3] and S. K. Maurya[4]

[1]Department of Physics, National Defence Academy, Pune, India, [2]Department of Mathematics, Jadavpur University, Kolkata, India, [3]Department of Physics, The Institute of Mathematical Sciences, Chennai, Tamil Nadu, India, [4]Department of Mathematical and Physical Sciences, College of Arts and Sciences, University of Nizwa, Nizwa, Sultanate of Oman

This paper supplements the article (Eur. Phys. J. C 76: 246, 2016) by extending some more new wormhole solutions in the background of Finslerian geometry. Here, we present six more solutions by considering i) a linear equation of state (EoS) $p_r = \omega\rho$ and three different shape functions, ii) a linear relationship between radial and tangential pressure as $p_t = np_r$ with two different redshift functions and iii) a specific density profile with a linear equation of state $p_r = \omega\rho$. It is found that all these wormholes are violating null energy condition (NEC) signifying that the throats are opened by exotic matters. Since the equation of state parameters, $\omega$ or $\omega_r = p_r/\rho$ for all the solutions are $< -1$, the corresponding exotic matter is none other than the phantom energy. Further, the two solutions in Case ii) are not asymptotically flat since $\lim_{r\to\infty}[b(r)/r] \nrightarrow 0$. To make it asymptotically flat we matched it with the Schwarzschild vacuum.

KEYWORDS

**Finsler geometry, wormholes, energy conditions, phantom energy, embedding diagram**

## 1 Introduction

Two distinct spacetimes are possible to be connected through a shortcut, which arises due to the hypothetical topological behavior of spacetime, popularly known as "wormhole". It is interesting to note that in their work Fuller and Wheeler [1], first coined the term wormhole and provided due credit to Weyl [2] for the fundamental idea of the possibility of non-simply connected spacetime. However, according to few researchers, the study of the wormhole was actually initiated by Flamm [3]. Later an important study by Einstein and Rosen revealed the wormhole geometry popularly known as the Einstein-Rosen bridge where they investigated the non-singular coordinate patches of the Reissner-Nordström and the Schwarzschild solutions. Clearly, these two fundamental ideas of wormholes are completely different from each other. The wormholes, which are offspring of the eternal black hole solution, are not suitable for transferring information, and they are actually non-traversable in their nature. On the other hand, the idea of a wormhole due to the non-simply connected nature of spacetime as endorsed by Weyl predicts the presence of electromagnetic field

lines without a source, which actually possible to be used as a classical communication channel.

With the proposal of the idea of a wormhole, researchers showed great curiosity about whether it is possible to construct a sustainable wormhole, the topological tunnel of space, and whether will it be consistent with the laws of physics. In 1962 in his seminal work Wheeler [4] predicted the Reissner-Nordström and Kerr wormhole geometries in the form of quantum foam at the Planck scale. In the further study by Hawking [7] these wormholes have been featured as "Euclidean wormholes" which are not traversable. With the suitable choice of topology this wormhole geometry which is described by the Schwarzschild metric [4], contains the horizon and it is impossible to traverse through them as its throat squeezes very quickly [5]. Hence, it is obvious to consider the presence of non-zero stress and energy to support the configuration of the wormhole throat [6]. This endorses the presence of the material near the throat that must have a radial tension greater than its mass-energy density which property has not been seen so far in any material. In their detailed study, Morris et al. [8] successfully explained static and spherically symmetric traversable wormholes which support the presence of such exotic matter that violates the energy conditions. Immediately questions arise such as i) Is it admissible by quantum field theory to consider such type of stress-energy tensor to maintain a two-way traversable wormhole? ii) Whether is it possible to form a wormhole that arises due to the non-simply connected nature of spacetime as it is not the usual case of spatial sections of the wormhole? These questions should be answered as the laws of physics must be consistent with the physics of traversable wormholes. In fact, a traversable wormhole may act like a "time machine", which in that case may violate the causality [9].

In their studies, different researchers have confirmed that it is necessary to consider exotic matter around the throat of the static wormhole configurations, which also guarantees the violation of the null energy condition (NEC). Although an important letter by Visser et al. [10] reveals that though it is essential to violate averaged null energy condition (ANEC), but it is enough to have the presence of ANEC-violating matter infinitesimally small. It is worth mentioning that the solutions of the static configuration of wormholes are studied in literature [10–16] must be consistent with some property to be traversable. However, to understand the extensive delineation of the physical aspects of wormholes, we suggest readers to study different wormhole configurations such as rotating wormholes [17, 18], dynamical wormholes [19, 20], wormholes with a cosmological constant $\Lambda$ [21, 22], etc. Matters violating the energy conditions can be categorized by the equation of state parameter $\omega = p/\rho$. The strong energy condition demands $\omega \geq -1/3$ for normal fluids and becomes exotic fluids (dark energy) if $\omega < -1/3$. The cosmological constant corresponds to $\omega = -1$, phantom $\omega < -1$ and quintessence $-1 < \omega < -1/3$. Since opening the throat of a wormhole requires the violation of null energy condition, i.e. $\rho+p < 0$ demands $\omega < -1$, the throat can be open either by phantom energy or cosmological constant. Many authors presented wormhole solutions supported by exotic matters in GR and modified gravity [23–27].

Investigation of the different properties of spacetime in more generalized theories of gravity has attracted much attention among scientists in recent days. Interestingly, most of the articles are concerned with the geometrical aspect of the field equation. Also, recent observational evidence has triggered the search for a more generalized form of gravitational theory compared to general relativity (GR). In fact, with the advancements of quantum gravity research, many investigations came up with the idea that GR is actually embedded in some more generalized form of the gravity field. Besides the astrophysical significance, there are many possible applications of spacetime in ADS/CFT correspondence, string theory, induced gravity, and de Sitter gauge theory [28, 29].

Importantly based on the following reasons, it is suitable to choose Finsler geometry over GR are given by i) the geometry is dependent on the dynamics as well as the position of the system, and no quadratic restrictions are required to bound the length element in Finsler geometry [30]. The measurement of time between two events that appeared to an observer is actually the same as the distance between two events that occurred in the world line of the same observer. ii) The measurement depends on the tangent bundle of a homogeneous function which results that the arcs depending on length as well as velocity. iii) Also, one can easily resolve by considering $F(x, y) = \sqrt{g_{\mu\nu} y^{\mu} y^{\nu}}$ in Riemannian manifold $(M, g_{\mu\nu}(x))$ the present Finsler space which is quadratic in terms of $y^{\theta}$ and $y^{\phi}$. In fact, the covariant derivative of the Riemannian space is possible to be used in this present case as it is a semi-definite Finsler space. Hence, the Bianchi identity in this Finsler space is the same as found in the Riemannian space. The gravitational field equations are found as the present Finsler space reduces into the Riemannian space.

A detailed study of Einstein's gravity in the framework of Finslerian geometry is found in the literature [31–34]. Also, in several recent articles [35–42] researchers have studied anisotropy of the Universe and the violation of Lorentzian invariance in Finsler geometry. Further, in the framework of Finsler geometry Minguzzi [43] has studied the singularity theorem and the Raychaudhuri equation. In their important study, Stavrinos and Alexious [44] have studied scalar-tensor theory and the generalized form of Raychaudhuri equation in the Finsler-Rander spacetime. Aazami and Javaloyes [45] have studied Penrose's singularity theorem in Finslerian geometry. Rahaman et al. [46] and Chowdhuri et al. [47] have presented an important study on the compact stars model in Finsler spacetime. On the other hand, the investigation made by Li [48] provides the eigenfunction of the Finslerian Laplacian

operator and also features Finslerian Reissner-Nordström solution for vacuum. Li and Chang [49] also presented the exact vacuum solution in Finsler spacetime. Other traversable wormholes are also presented by many authors in various modified gravity theories [50, 51]. Övgün and Sakalli presented a thin shell wormhole solution using Visser cut and paste technique [52], gravitino and vector particles as Hawking radiation from the traversable Lorentzian wormholes [53, 54], the deflection angle of light by wormholes [55]. A model of cosmic springs in Finslerian geometries was also presented by Lake [56].

## 2 Finslerian geometry and wormhole field equations

The Finslerian geometry is constructed from Finsler structure $F$ which is defined as [57]

$$(x, \mu y) = \mu F(x, y) \quad \forall \quad \mu > 0. \tag{1}$$

Here $x \in M$ represents position and $y = dx/dt$, the velocity. The metric describing Finslerian geometry is given as [58]

$$g_{\mu\nu} \equiv \frac{\partial}{\partial y^{\mu}} \frac{\partial}{\partial y^{\nu}} \left(\frac{1}{2} F^2\right). \tag{2}$$

The geodesic equation in the Finsler manifold is expressed as [58]

$$\frac{d^2 x^{\mu}}{d\tau^2} + 2G^{\mu} = 0, \tag{3}$$

where $G^{\mu}$ is called the geodesic spray coefficients defined as [58]

$$G^{\mu} = \frac{1}{4} g^{\mu\nu} \left(\frac{\partial^2 F^2}{\partial x^{\lambda} \partial y^{\nu}} y^{\lambda} - \frac{\partial F^2}{\partial x^{\nu}}\right). \tag{4}$$

The Ricci scalar in Finsler geometry is written as [58]

$$\mathcal{R} \equiv R^{\mu}_{\mu} = \frac{1}{F^2} \left(2\frac{\partial G^{\mu}}{\partial x^{\mu}} - y^{\lambda} \frac{\partial^2 G^{\mu}}{\partial x^{\lambda} \partial y^{\mu}} + 2G^{\lambda} \frac{\partial^2 G^{\mu}}{\partial x^{\lambda} \partial y^{\mu}} - \frac{\partial G^{\mu}}{\partial y^{\lambda}} \frac{\partial G^{\lambda}}{\partial y^{\mu}}\right) \tag{5}$$

$$R^{\mu}_{\nu} = \frac{1}{F^2} R^{\mu}_{\lambda\nu\rho} y^{\lambda} y^{\rho}. \tag{6}$$

Here $R^{\mu}_{\lambda\nu\rho}$ depends on connection and $R^{\mu}_{\nu}$ depends only on the Finsler structure $F$.

Due to Birkhoff's theorem, it is well-known that most of static vacuum solutions are reducible to the Schwarzschild's form, hence we will assume the Finsler structure in the similar form

$$F^2 = B(r) y^t y^t - A(r) y^r y^r - r^2 \bar{F}^2 \left(\theta, \phi, y^{\theta}, y^{\phi}\right). \tag{7}$$

The Finsler metric is given below

$$g_{\mu\nu} = \mathrm{diag}\left(B, -A, -r^2 \bar{g}_{ij}\right), \tag{8}$$

$$g^{\mu\nu} = \mathrm{diag}\left(B^{-1}, -A^{-1}, -r^2 \bar{g}^{ij}\right), \tag{9}$$

Where $\bar{g}^{ij}$ are derived from $\bar{F}^2$ and $(\theta, \phi) \equiv (i, j)$. The components of the geodesic spray coefficient become

$$G^t = \frac{B'}{2B} y^t y^r, \tag{10}$$

$$G^r = \frac{A'}{4A} y^r y^r + \frac{B'}{4A} y^t y^t - \frac{r}{2A} \bar{F}^2, \tag{11}$$

$$G^{\theta} = \frac{1}{r} y^{\theta} y^r + \bar{G}^{\theta}, \tag{12}$$

$$G^{\phi} = \frac{1}{r} y^{\phi} y^r + \bar{G}^{\phi}, \tag{13}$$

Where the prime represents differentiation with respect to $r$ and the $\bar{G}$ is the geodesic spray coefficients derived by $\bar{F}$. Substituting (Eq. 10)-(Eq. 13) to (Eq. 5) we the expression of Ricci scalar as

$$\begin{aligned} F^2 \mathcal{R} = &\left[\frac{B''}{2A} - \frac{B'}{4A}\left(\frac{A'}{A} + \frac{B'}{B}\right) + \frac{B'}{rA}\right] y^t y^t \\ &+ \left[-\frac{B''}{2B} + \frac{B'}{4B}\left(\frac{A'}{A} + \frac{B'}{B}\right) + \frac{A'}{rA}\right] y^r y^r \\ &+ \left[\bar{\mathcal{R}} - \frac{1}{A} + \frac{r}{2A}\left(\frac{A'}{A} - \frac{B'}{B}\right)\right] \bar{F}^2, \end{aligned} \tag{14}$$

where $\bar{\mathcal{R}}$ denotes the Ricci scalar correspond to $\bar{F}$.

Akbar-Zadeh [59] first introduced the notion of Ricci tensor in the Finsler geometry as

$$\mathcal{R}_{\mu\nu} = \frac{\partial^2}{\partial y^{\mu} \partial y^{\nu}} \left(\frac{1}{2} F^2 \mathcal{R}\right). \tag{15}$$

The scalar curvature in the Finsler geometry is defined as $S = g^{\mu\nu} \mathcal{R}_{\mu\nu}$. Now the modified Einstein's tensor is given by (See Appendix A)

$$G_{\mu\nu} \equiv \mathcal{R}_{\mu\nu} - \frac{1}{2} g_{\mu\nu} S. \tag{16}$$

The covariant conservation of $G_{\mu\nu}$ in Finsler geometry i.e., $G^{\mu}_{\nu;\mu} = 0$ was proved by Chang and Li [37].

Now we can write the components of Einstein's tensor in Finsler geometry as

$$G^t_t = \frac{A'}{rA^2} - \frac{1}{r^2 A} + \frac{\lambda}{r^2}, \tag{17}$$

$$G^r_r = -\frac{B'}{rAB} - \frac{1}{r^2 A} + \frac{\lambda}{r^2}, \tag{18}$$

$$G^{\theta}_{\theta} = G^{\phi}_{\phi} = -\frac{B''}{2AB} - \frac{B'}{2rAB} + \frac{A'}{2rA^2} + \frac{B'}{4AB}\left(\frac{A'}{A} + \frac{B'}{B}\right). \tag{19}$$

Finally, we can write the field equations in Finsler spacetime as

$$G^{\mu}_{\nu} = 8\pi_F T^{\mu}_{\nu}, \tag{20}$$

with $T^{\mu}_{\nu}$ is the energy-momentum tensor and $4\pi_F$ is expressing the volume of $\bar{F}$ in the field equation.

Assuming a matter distribution with anisotropic pressure, the form of the energy-momentum tensor can be written as

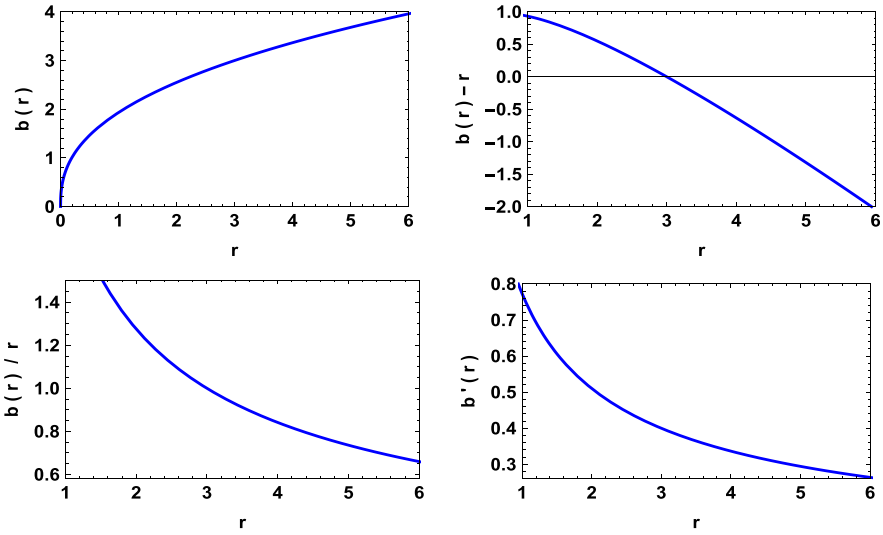


FIGURE 1
Variation of $b$, $b-2$, $b/r$ and $b'(r)$ for model I with $a = 3$, $\lambda = 1.2$, $\omega = -2$ and $n = 0.4$.

$$T^{\mu}_{\xi} = \rho v^{\mu} v_{\xi} + p_r \chi_{\xi} \chi^{\mu} + p_t \left( v^{\mu} v_{\xi} - \chi_{\xi} \chi^{\mu} + g^{\mu}_{\xi} \right), \tag{21}$$

where $v^{\mu} v_{\mu} = -\chi^{\mu} \chi_{\mu} = 1$, $p_r$ and $p_t$ denote radial and transverse pressures, respectively. $\rho$ is the density of the fluid distribution, $v^{\mu}$ is the four velocity, and $\chi^{\mu}$ is the unit space-like vector in the radial direction.

By using the energy-momentum tensor in (Eq. 21) along with the field Eq. 20 we get.

$$8\pi_F \rho = \frac{A'}{2A^2} - \frac{1}{r^2 A} + \frac{\lambda}{r^2}, \tag{22}$$

$$8\pi_F p_r = \frac{B'}{rAB} + \frac{1}{r^2 A} - \frac{\lambda}{r^2}, \tag{23}$$

$$8\pi_F p_t = \frac{B''}{2AB} + \frac{B'}{2rAB} - \frac{A'}{2rA^2} - \frac{B'}{4AB}\left( \frac{A'}{A} + \frac{B'}{B} \right), \tag{24}$$

With $\lambda$, the constant flag curvature. Now the Finsler form of the Morris-Thorne [6] wormhole geometry can be written as

$$F^2 = -e^{2f(r)} y^t y^t + \frac{y^r y^r}{1 - \frac{b}{r}} + r^2 \bar{F}^2 \left( \theta, \phi, y^{\theta}, y^{\phi} \right), \tag{25}$$

where $y^i = di/d\tau$. And the 2-surface $\bar{F}^2$ is taken as

$$\bar{F}^2 = y^{\theta} y^{\theta} + f(\theta, \phi)\ y^{\phi} y^{\phi} \tag{26}$$

with the corresponding metric $\bar{g}_{ij} = \mathrm{diag}(1, f(\theta, \phi))$. To get vanishing off-diagonal components of $F^2 \mathcal{R}$ in (Eq. 14) the function $f(\theta, \phi) = f(\theta)$ and one of the possible choice that preserves the spherical symmetry is $f(\theta) = \sin^2(\sqrt{\lambda}\ \theta)$. Hence, the final form of the Finsler-Morris-Thorne wormhole geometry can be written as

$$F^2 = -e^{2f(r)} y^t y^t + \frac{y^r y^r}{1 - \frac{b}{r}} + r^2 \left( y^{\theta} y^{\theta} + \sin^2\left( \sqrt{\lambda}\ \theta \right) \right) y^{\phi} y^{\phi} \tag{27}$$

The Finslerian field (Eq. 22, Eq. 24) reduce to

$$8\pi_F \rho = \frac{b' + \lambda - 1}{r^2}, \tag{28}$$

$$8\pi_F p_r = \left( 1 - \frac{b}{r} \right) \left( \frac{2f'}{r} + \frac{1}{r^2} \right) - \frac{\lambda}{r^2}, \tag{29}$$

$$8\pi_F p_t = \left[ 1 - \frac{b}{r} \right] \left[ f'' + \frac{f'}{r} + f'^2 \right] - \left[ \frac{b'}{r} - \frac{b}{r^2} \right] \left[ \frac{f'}{2} + \frac{1}{2r} \right]. \tag{30}$$

Here, $b(r)$ and $f(r)$ are shape-function and redshift functions respectively. To solve the above field equations, we need extra information to integrate further. To solve the above field equations we will adopt few techniques i.e., assuming specific equation of state, well-known wormhole shape function and redshift function or assuming $p_r$ & $p_t$ relationship.

## 3 Finslerian wormholes with linear equation of state

In these cases, we will assume a linear equation of state of the form $p_r = \omega\rho$ along with a specific choice of shape functions.

### 3.1 Model I: $b(r) = a(r/a)^n$

Considering this shape function along with the linear EoS, the field equations can be integrated to yield the red-shift function as

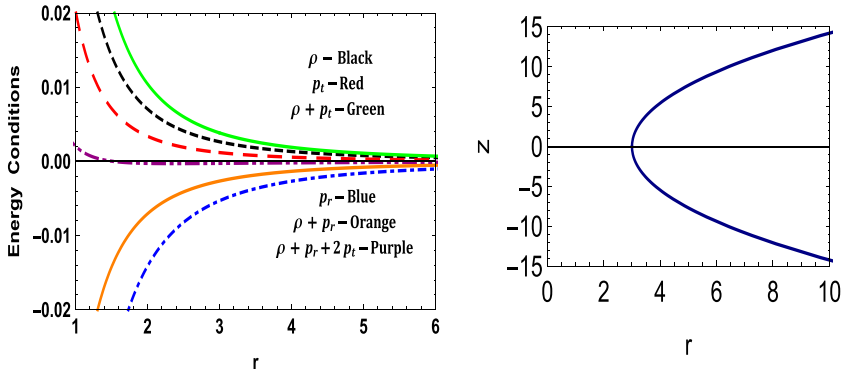


FIGURE 2
Variation of energy conditions and embedding diagram for the model I with $a = 3$, $\lambda = 1.2$, $\omega = -2$ and $n = 0.4$.

$$f(r) = A + \frac{1}{2(n-1)}\left[\log(r)\{n(\lambda\omega+\lambda-1)+1\} - \{\lambda(\omega+1) + (n-1)\omega\}\log\left\{r - a\left(\frac{r}{a}\right)^n\right\}\right]. \quad (31)$$

Here $A$ is the constant of integration. Therefore, the density and pressure take the forms

$$8\pi_F\rho = \frac{n(r/a)^{n-1} + \lambda - 1}{r^2}, \quad (32)$$

$$8\pi_F p_r = \frac{\omega}{r^2}\left[n\left(\frac{r}{a}\right)^{n-1} + \lambda - 1\right], \quad (33)$$

$$8\pi_F p_t = \frac{1}{4r^3[r - a(r/a)^n]}\left[a^2 n\{n\omega^2 - (n-3)\omega + 1\}\left(\frac{r}{a}\right)^{2n} + ar\left(\frac{r}{a}\right)^n\{(\lambda-1)(\omega+1) + 2n^2\omega + n(2\lambda\omega^2 + 3\lambda\omega + \lambda - 2\omega^2 - 5\omega - 1)\} + (\lambda-1)^2 r^2(\omega+1)^2\right]. \quad (34)$$

The rest of the quantities can be calculated from the above physical quantities. The quantity $a$ is the throat radius of the wormhole. The variations of all these parameters can be shown in Figures 1, 2. Now we can see that the throat is at $a = 5$ and is asymptotically flat. Now, since NEC is violated, i.e. $\rho+p_r < 0$, the throat is supported by exotic matter or precisely by phantom energy ($\omega < -1$). The revolution of the embedded surface can be seen in Figure 3.

## 3.2 Model II: $b(r) = a^3 c \log(a/r) + a$

For this shape function in the linear EoS, the field equations lead to

$$f'(r) = \frac{a^3 c\log\left(\frac{a}{r}\right) - a^3 c\ \omega + a + r(\lambda-1)(\omega+1)}{2r\left(r - a^3 c\log\left(\frac{a}{r}\right) - a\right)}, \quad (35)$$

which is not exactly integrable, however, one can always find the related physical quantities as they are dependent only on their derivatives. Here the physical parameters take the form

$$8\pi_F\rho = \frac{\lambda r - a^3 c - r}{r^3}, \quad (36)$$

$$8\pi_F p_r = \frac{\omega(\lambda r - a^3 c - r)}{r^3}, \quad (37)$$

$$8\pi_F p_t = \frac{1}{4r^3\left(r - a^3 c\log\left(\frac{a}{r}\right) - a\right)}\left[a^6 c^2\omega(\omega+1) - a^4(3c\omega + c) - a^3 cr(2\lambda\omega^2 + 3\lambda\omega + \lambda - 2\omega^2 - 5\omega - 1) - a^3 c\log\left(\frac{a}{r}\right)[a^3(3c\omega + c) - r(\lambda-1)(\omega+1)] + ar(\lambda-1)(\omega+1) + (\lambda-1)^2 r^2(\omega+1)^2\right]. \quad (38)$$

Now the energy conditions etc., can be calculated using the above expressions. Further, the variations of these physical parameters can be seen in Figures 4, 5. The throat radius is found to be 2 km and is opened by phantom energy.

## 3.3 Model III: $b(r) = ac(1 - a/r) + a$

The solution, in this case, is found to be

$$f(r) = D + [-\log(r-a)[(c-1)\omega + \lambda(\omega+1)] + [c(\lambda\omega + \lambda - \omega) + \omega]\log(r - ac) + (c-1)(\omega-1)\log(r)]. \quad (39)$$

Further, the physical quantities are found to be

$$8\pi_F\rho = \frac{a^2 c/r^2 + \lambda - 1}{r^2}, \quad (40)$$

$$8\pi_F p_r = \frac{\omega(a^2 c/r^2 + \lambda - 1)}{r^2}, \quad (41)$$

$$8\pi_F p_t = \frac{1}{4r^4(a-r)(ac-r)}\left[a^4 c^2(\omega^2 - 4\omega - 1) + a^3 cr(c+1)(5\omega+1) + 2a^2 cr^2\omega \times(\lambda\omega + \lambda - \omega - 3) + a(c+1)(\lambda-1)r^3(\omega+1) + (\lambda-1)^2 r^4(\omega+1)^2\right]. \quad (42)$$

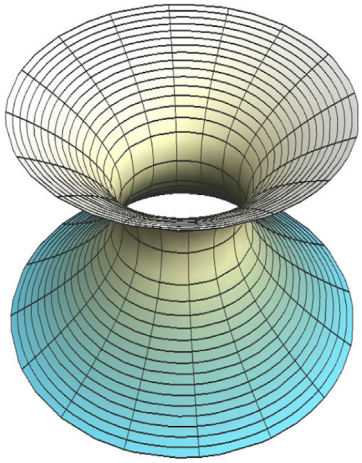

FIGURE 3
Surface revolution of embedding diagram for model I.

The variations of these physical quantities are given in Figures 6, 7. Here also, the NEC is violated, and therefore the WH throat is supported by the exotic matter which is found to be phantom energy. The revolution of the embedded surface can be seen in Figure 8.

## 4 Finslerian wormholes with $p_t = np_r$

Unlike the first method we have adopted above, we would like to extend our investigation by assuming a linear relationship between the tangential and radial pressure as $p_t = np_r$, where $n$ can be treated as an anisotropic parameter. To solve the field equations, further we ansatz different forms of $f(r)$.

### 4.1 Model IV: $f(r) = c$

For the initial assumptions $p_t = np_r$ and $f(r) = c$, the resulting solution is

$$b = r\left(Hr^{2n} - \lambda + 1\right), \tag{43}$$

with $H$ as the constant of integration. Here one can clearly see that this solution is not asymptotically flat since $\lim_{r\to\infty}[b(r)/r] \nrightarrow 0$. To make it asymptotically flat we must match it with exterior Schwarzschild spacetime. The matching equation can be written as

$$e^{2f(R)} = 1 - \frac{2\mathcal{M}}{R} = 1 - \frac{b(R)}{R}, \tag{44}$$

where $R$ is the surface when the two spacetimes meet. Using (Eq. 44), we get

$$b(R) = R\left(HR^{2n} - \lambda + 1\right) = 2\mathcal{M} \tag{45}$$

$$R = 2\mathcal{M}\left(1 - e^{2c}\right)^{-1}, \tag{46}$$

Which leads to a constraint on the constants $H$ and $c$ as

$$c = \ln\left\{\lambda - H\left[2\mathcal{M}\left(1 - e^{2c}\right)^{-1}\right]^{2n}\right\}^{1/2}. \tag{47}$$

Now the density, pressures, and energy conditions are given by

$$8\pi_F\rho = \frac{Hr^{2n} + 2Hnr^{2n}}{r^2}, \tag{48}$$

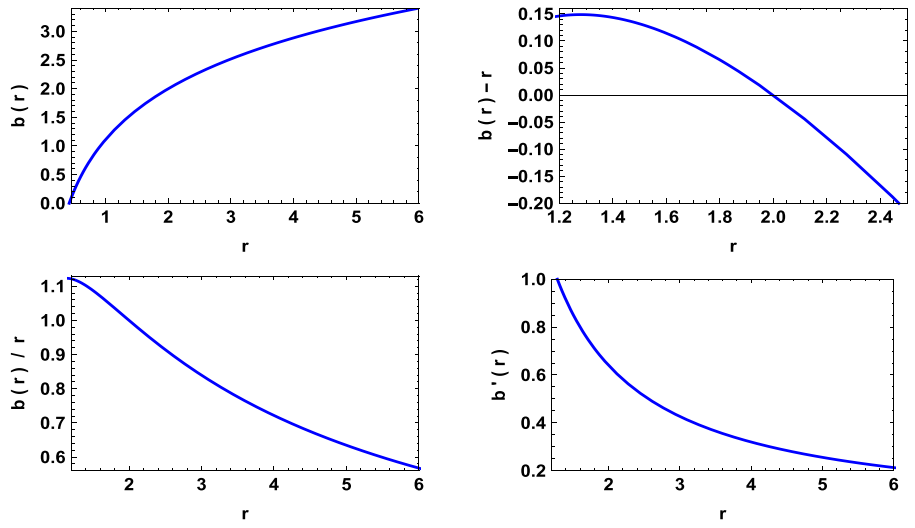


FIGURE 4
Variation of $b$, $b-2$, $b/r$ and $b'(r)$ for model II with $a = 2$, $\lambda = 1.2$, $\omega = -2$, $c = -0.16$.

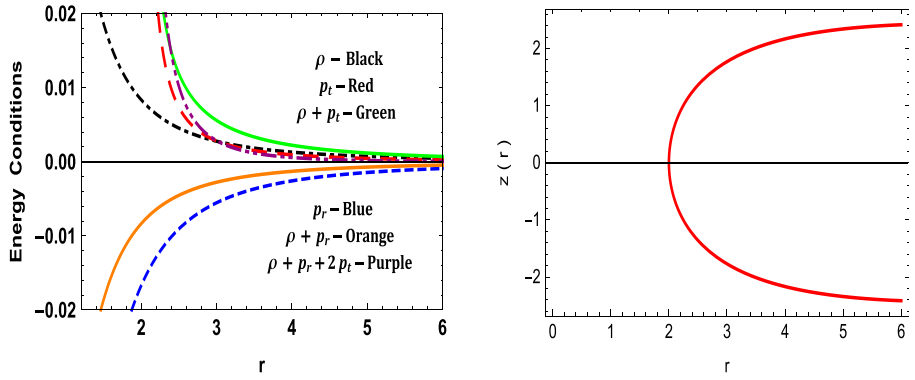


FIGURE 5
Variation of energy conditions and embedding surface for model II with $a = 2$, $\lambda = 1.2$, $\omega = -2$, $c = -0.16$.

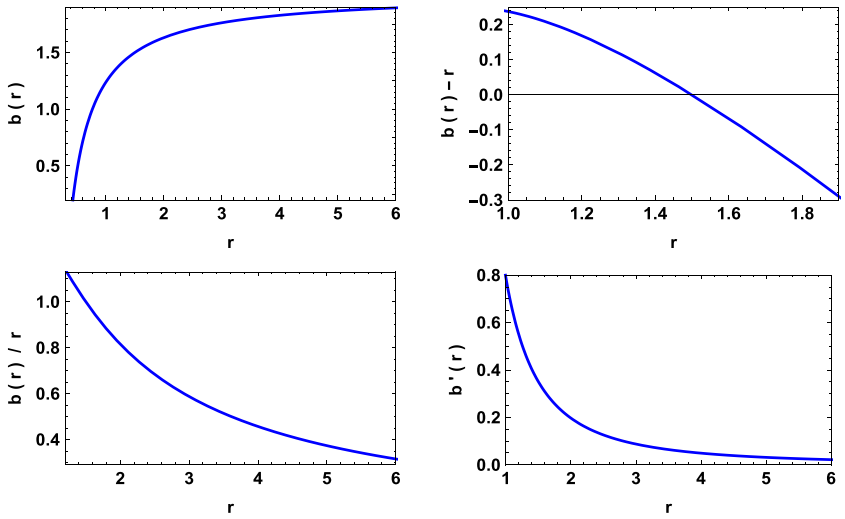


FIGURE 6
Variation of $b$, $b-2$, $b/r$ and $b'(r)$ for model III with $a = 1.5$, $\lambda = 1.2$, $\omega = -2$, $c = 0.35$.

$$8\pi_F p_r = -Hr^{2n-2}, \tag{49}$$

$$8\pi_F p_t = -Hnr^{2n-2}, \tag{50}$$

$$8\pi_F (\rho + p_r) = 2Hnr^{2n-2}, \tag{51}$$

$$8\pi_F (\rho + p_t) = H(n+1)r^{2n-2}, \tag{52}$$

$$8\pi_F (\rho + p_r + 2p_t) = 0. \tag{53}$$

The variations of $b(r)$, $b'(r)$ and $b(r) - r$ is given in Figure 9. The variations of $p_r$, $p_t$, and energy density can be seen in Figure 10. Here we can see that the throat radii are the same for all the EoS parameters $\omega = -4.98, -2.5, -1.66, -1.24$. Again, the NEC is violated, and the corresponding EoS parameter $\omega_r = p_r/\rho$ is less than $-1$ thereby, the WH is supported by phantom energy. The surface revolution of the embedded surface is shown in Figure 11.

## 4.2 Model V: $f(r) = \log(r/\gamma)$

For this redshift function, one can find the solution as

$$b(r) = Mr^{3n} + \frac{(\lambda - 3)nr + r}{1 - 3n}, \tag{54}$$

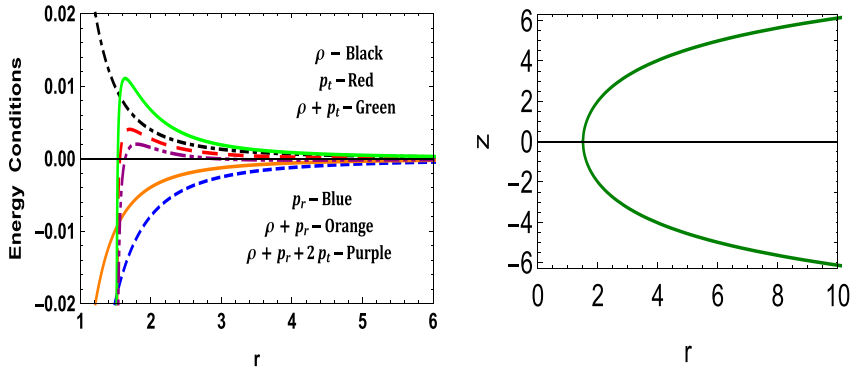


FIGURE 7
Variation of energy conditions and embedding surface for model III with $a = 1.5$, $\lambda = 1.2$, $\omega = -2$, $c = 0.35$.

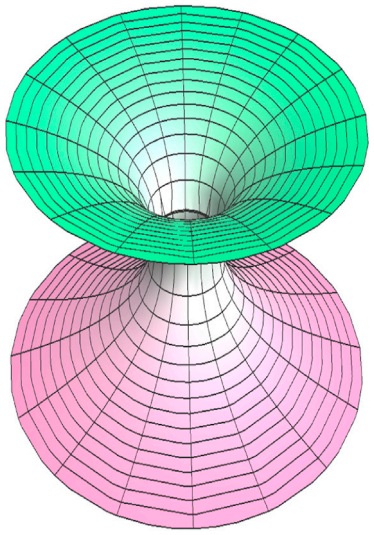

FIGURE 8
Surface revolution of embedding diagram for model III.

where $M$ is the constant of integration. Again, this solution is not asymptotically flat due to $\lim_{r\to\infty}[b(r)/r] \nrightarrow 0$, so we have to match this interior spacetime with exterior Schwarzschild spacetime. Further, using (Eq. 44) we get

$$R = \frac{3^{2/3}\gamma^2 + \sqrt[3]{3}\, a_1^{2/3}}{3\, a_1^{1/3}} \tag{55}$$

$$b(R) = 2\mathcal{M} = R\left[MR^{3n-1} + \frac{(\lambda-3)n+1}{1-3n}\right]. \tag{56}$$

These above equations lead to a constraint given as

$$2\mathcal{M} = \frac{3^{2/3}\gamma^2 + \sqrt[3]{3}\, a_1^{2/3}}{3\, a_1^{1/3}}\left[M\left(\frac{3^{2/3}\gamma^2 + \sqrt[3]{3}\, a_1^{2/3}}{3\, a_1^{1/3}}\right)^{3n-1} + \frac{(\lambda-3)n+1}{1-3n}\right], \tag{57}$$

where,

$$a_1 = \sqrt{81\gamma^4\mathcal{M}^2 - 3\gamma^6} - 9\gamma^2\mathcal{M}. \tag{58}$$

Now the density and pressure take form

$$8\pi_F\rho = \frac{\lambda + 3Mnr^{3n-1} + \frac{(\lambda-3)n+1}{1-3n} - 1}{r^2}, \tag{59}$$

$$8\pi_F p_r = \frac{1}{r^3}\left(\frac{\lambda r}{3n-1} - 3Mr^{3n}\right), \tag{60}$$

$$8\pi_F p_t = \frac{n}{r^3}\left(\frac{\lambda r}{3n-1} - 3Mr^{3n}\right), \tag{61}$$

And the energy conditions take the very simple forms

$$\rho + p_r = \frac{3M\left(3n^2 - 4n + 1\right)r^{3n} + 2\lambda nr}{8\pi_F\left(3n-1\right)r^3}, \tag{62}$$

$$\rho + p_t = \frac{\lambda}{8\pi_F r^2}, \tag{63}$$

$$\rho + p_r + 2p_t = \frac{4\lambda nr - 3M\left(3n^2 + 2n - 1\right)r^{3n}}{8\pi_F\left(3n-1\right)r^3}. \tag{64}$$

The variations of pressure, density, energy conditions, etc. are shown in Figures 12, 13. Here one can observe that the throat radius depends on the parameter $n$ for which the $r_{th}$ is smaller for $n = -1$ and larger for $n = -0.07$. Further, EoS parameter $\omega$ also increases when $n$ increases leading to more exotic matter and thereby wider throat radius. Further, the violation of NEC and $\omega_r = p_r/\rho < -1$ shows that the matter is exotic (phantom energy).

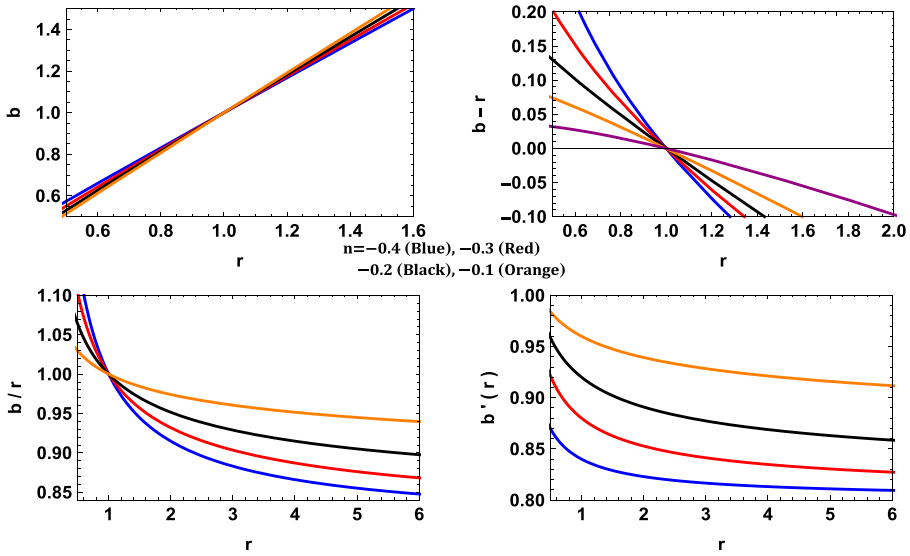


FIGURE 9
Variation of $b$, $b-2$, $b/r$ and $b'(r)$ for model IV with $H = 0.2$, $\lambda = 0.2$.

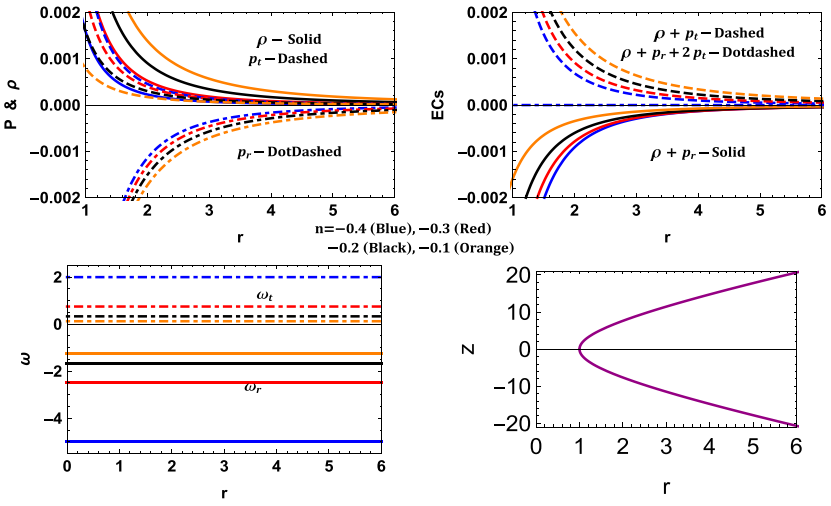


FIGURE 10
Variation of energy conditions and embedding surface for model IV with $H = 0.2$, $\lambda = 0.2$.

## 5 Finslerian wormholes with specific density profile and a linear EoS (model VI)

To find the third category of solutions, we will assume a specific density profile with a linear equation of state of the form

$$\rho = c\left(\frac{a}{r}\right)^{\alpha}, \quad p_r = \omega\rho. \tag{65}$$

From the first relation with the field equation, we get

$$b(r) = \frac{cr^3}{3-\alpha}\left(\frac{a}{r}\right)^{\alpha} + F - \lambda r + r, \tag{66}$$

where $F$ is the constant of integration. Since the expression of the shape function doesn't include $\omega$, its throat will not be affected by EoS parameter. And the linear EoS with the density profile after using the field equations and the above $b(r)$, we can find $f'(r)$ as

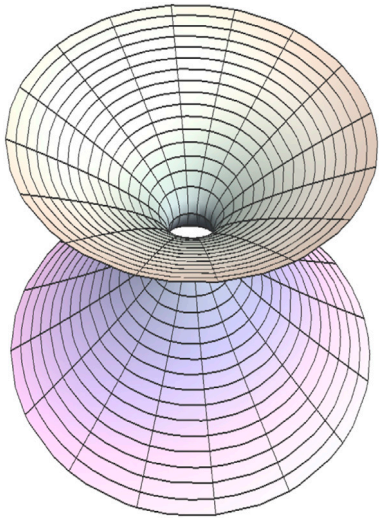

FIGURE 11
Surface revolution of embedding diagram for model IV.

$$f'(r) = \frac{cr^3[(\alpha-3)\omega-1]\left(\frac{a}{r}\right)^{\alpha} + (\alpha-3)F}{2r\left(cr^3\left[\frac{a}{r}\right]^{\alpha} - (\alpha-3)F + (\alpha-3)\lambda r\right]}. \tag{67}$$

Which is not exactly integrable. Although, one can find the physical parameters as

$$8\pi_F\rho = \frac{1}{r^2}\left[\frac{3cr^2(a/r)^{\alpha}}{3-\alpha} - \frac{a\alpha cr(a/r)^{\alpha-1}}{3-\alpha}\right], \tag{68}$$

$$8\pi_F p_r = c\,\omega\left(\frac{a}{r}\right)^{\alpha}, \tag{69}$$

$$8\pi_F p_t = \frac{c(a/r)^{\alpha}}{4\left[cr^3\left(\frac{a}{r}\right)^{\alpha} - (\alpha-3)F + (\alpha-3)\lambda r\right]}\Big[cr^3(\alpha(\omega-1)\omega - 3\omega^2 - 1)\left(\frac{a}{r}\right)^{\alpha} + (\alpha-3)F[(2\alpha-3)\omega+1] - 2(\alpha^2-5\alpha+6)\lambda r\omega\Big]. \tag{70}$$

Figure 14 shows the behavior of the shape function and its related parameters. The trends of pressures, density and energy conditions are given in Figure 15, which shows that the NEC is again violated. The nature of the exotic matter can be known if we see the EoS parameter $\omega_r = p_r/\rho$. Here $\omega = -1.5$, i.e. less than −1, so again the exotic matter is phantom energy. The $r_{th}$ depends on the parameter $\alpha$, smaller values of $\alpha$ yields narrower throats and *vice versa*.

## 6 Construction of embedding diagrams

Considering a constant time slice i.e., $y^t = 0$ and in the 2-dimensional Finsler space $\bar{F}^2$ if one chooses $\theta = (\pi/2\sqrt{\lambda})$ (hence $y^{\theta} = d\theta/d\tau = 0$), then [Eq. 27] reduces to

$$F^2 = \frac{y^r y^r}{1-b/r} + r^2 y^{\phi} y^{\phi}. \tag{71}$$

If this Eq. 71 reduces to a 3-D cylindrical coordinate of the form

$$F^2 = y^z y^z + y^r y^r + r^2 y^{\phi} y^{\phi}, \tag{72}$$

than by comparing (Eq. 71) and (Eq. 72), the form of $z(r)$ can be found as

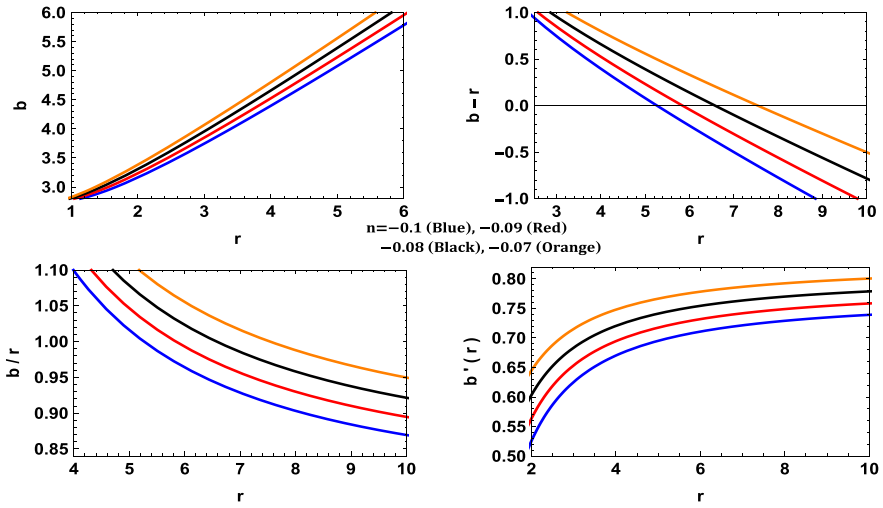


FIGURE 12
Variation of $b$, $b-2$, $b/r$ and $b'(r)$ for model V with $\lambda = 3$, $\gamma = 1.5$, $M = 2$.

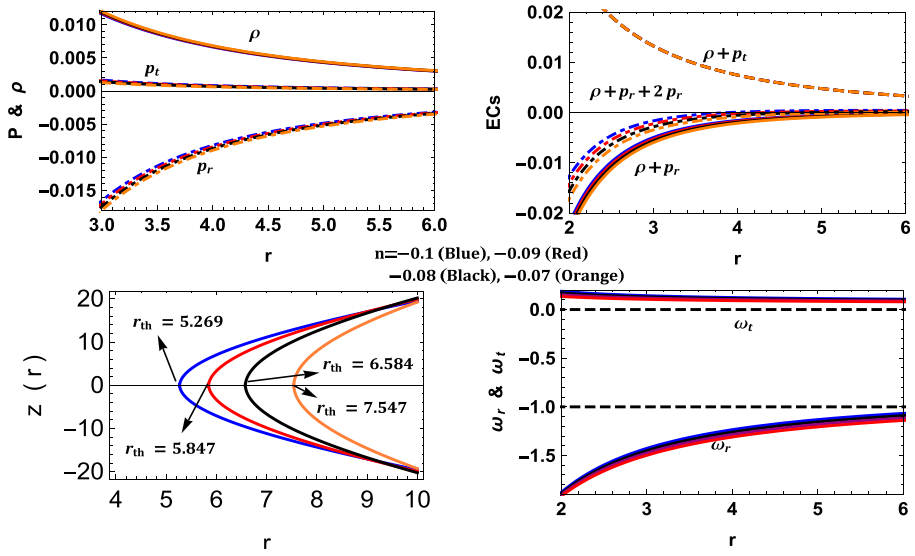


FIGURE 13
Variation of energy conditions and embedding surface for model V with $\lambda = 3$, $\gamma = 1.5$, $M = 2$.

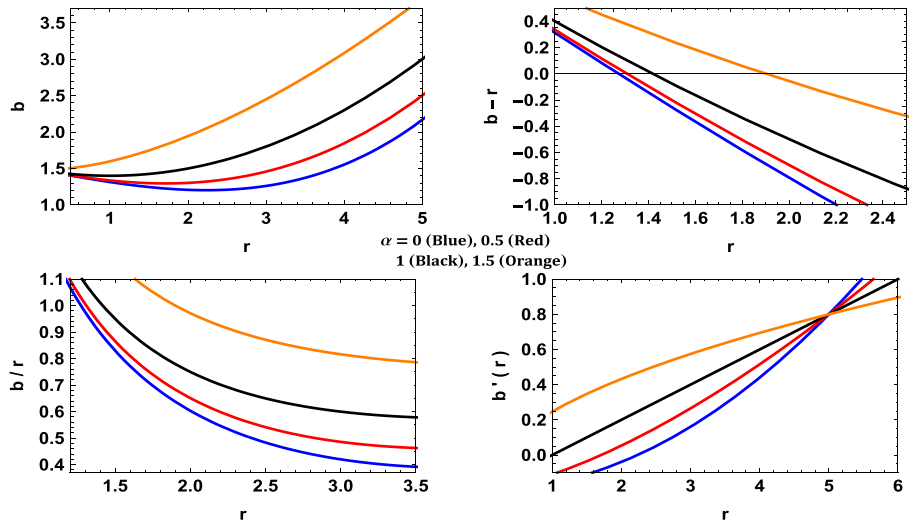


FIGURE 14
Variation of $b$, $b-2$, $b/r$ and $b'(r)$ for model VI with $c = 0.04$, $\lambda = 1.2$, $F = 1.5$, $a = 5$, $\omega = -1.5$.

$$\frac{y^r y^r}{1-b/r} = y^z y^z + y^r y^r \quad \text{or} \quad \frac{1}{1-b/r} = \frac{y^z y^z}{y^r y^r} + 1 = \left(\frac{dz/d\tau}{dr/d\tau}\right)^2 + 1$$
$$\Rightarrow \left(\frac{dz}{dr}\right)^2 + 1 = \left(1 - \frac{b}{r}\right)^{-1}. \tag{73}$$

On simplifying (Eq. 73) we get

$$\frac{dz}{dr} = \pm \frac{1}{\sqrt{r/b(r) - 1}} \quad \text{or} \quad z(r) = \pm \int \frac{dr}{\sqrt{r/b(r) - 1}}. \tag{74}$$

For model I, Eq. 74 is not integrable for the general case, however integrable for a given value of $n$. Further, for model II i.e., $b(r) = a^3 c \log(a/r) + a$ the embedding surface is not integrable exactly, thereby we used numerical integration to generate it. For model III the embedding surface can be integrated exactly and is given by

$$z(r) = \frac{2ar}{\sqrt{r-a}\sqrt{r-ac}} \sqrt{\frac{(r-a)(r-ac)}{r^2}} \left[(c+1)\log\left(\sqrt{r-ac} + \sqrt{r-a}\right) - \sqrt{c}\tanh^{-1}\left(\frac{\sqrt{c}\sqrt{r-a}}{\sqrt{r-ac}}\right)\right].$$

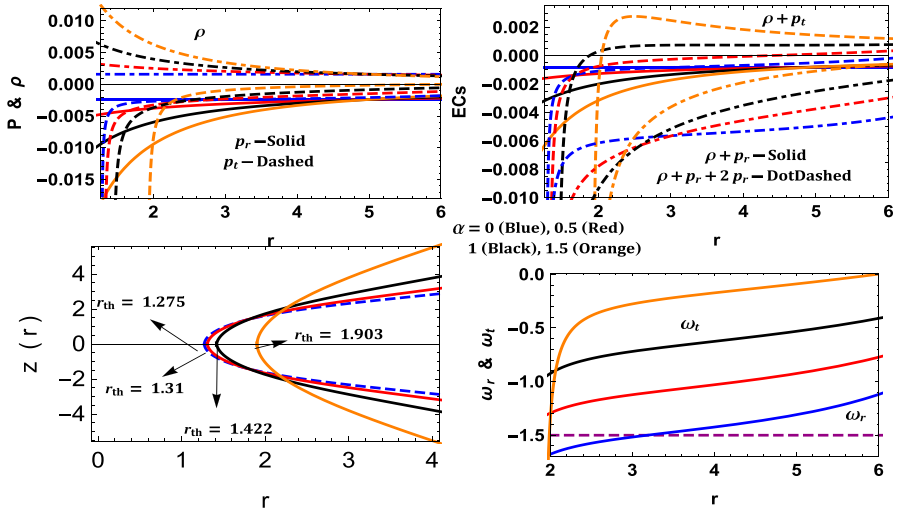


FIGURE 15
Variation of energy conditions and embedding surface for model VI with $c$ = 0.04, $\lambda$ = 1.2, $F$ = 1.5, $a$ = 5, $\omega$ = −1.5.

In a similar fashion, the embedding surface for model IV is found to be

$$z(r) = \frac{r}{(n+1)\sqrt{\lambda - Hr^{2n}}}\left[(1-\lambda n+n)\sqrt{1-\frac{Hr^{2n}}{\lambda}}\,{}_2F_1\left(\frac{1}{2},\frac{1}{2n};1+\frac{1}{2n};\frac{Hr^{2n}}{\lambda}\right)+Hr^{2n}-\lambda\right]. \tag{75}$$

Again, due to the non-integrability of Eq. 74 for model V and VI, we have used numerical integration to generate the 2-D embedding surface.

## 7 Results and discussions

In this work, we have presented six new wormhole (WH) solutions in Finslerian geometry. The first three models assumed a linear EoS along with specific forms of the shape function. The next two solutions were found by considering a linear relation between $p_r$ and $p_t$ through a constant parameter $n$. To close the system of equations, we have assumed two different redshift functions. Here the throat radius of WH IV depends on the redshift function only, however for the WH V, the $r_{th}$ depends on the anisotropic parameter $n$, i.e., more anisotropy makes the throat narrower and *vice versa*. Finally, the last solution was obtained *via* a linear EoS and a specific form of the density profile. In this case, the throat radius depends on density-related $\alpha$ parameter, more the density larger is the $r_{th}$.

Next, we have determined all the embedded surfaces for each WHs in 3D Euclidean space assuming an instant of time $t$ = constant and $\theta = (\pi/2\sqrt{\lambda})$. Models I, III, and IV only have exactly integrable embedding surfaces where we have also found their surface revolutions. The rest of the three WHs i.e., Models II, V, and VI were integrated numerically to generate the embedded surfaces. It is found that all these WH models are supported by exotic matter as the NEC is violated. The exact nature of these exotic matters can be found by analyzing the EoS parameter. All these cases yield $\omega = \omega_r = p_r/\rho < -1$ implying that the matter is simply phantom energy. It is also found that WHs III and IV were asymptotically non-flat i.e., $\lim_{r\to\infty}[b/r] \nrightarrow 0$. This problem has been resolved by matching the interior spacetime with the Schwarzschild vacuum. Further, it is also to be noted that Models I, II, III, and VI can have $\omega = -1$ (cosmological constant) with the flare-out conditions i.e., $b\,(r_{th}) = r_{th}$ & $b'(r_{th}) < 1$ and $b(r) < r$ for $r > r_{th}$ still holds. Overall, these new WH solutions might represent traversable wormholes.

## Data availability statement

The original contributions presented in the study are included in the article/supplementary material, further inquiries can be directed to the corresponding author.

## Author contributions

KNS conceptualized the manuscript including mathematical calculations, graph plotting, result analysis, and interpretations, FR did mathematical calculations and the resulting analysis, DD did the writing of the manuscript and interpretation of the results, SM did the editing, literature survey and the resulting analysis.

## Acknowledgments

KNS and FR are thankful to the authorities of the Inter-University Centre for Astronomy and Astrophysics, Pune, India for providing the research facilities.

## Conflict of interest

The authors declare that the research was conducted in the absence of any commercial or financial relationships that could be construed as a potential conflict of interest.

## Publisher's note



## References

1. Fuller RW, Wheeler JA. Causality and multiply connected space-time. *Phys Rev* (1962) 128:919–29. doi:10.1103/physrev.128.919

2. Weyl H. Feld und materie. *Ann Phys* (1921) 65:541–63. doi:10.1002/andp.19213701405

3. Flamm L. Beiträge zur einsteinschen gravitationstheorie. *Phys Z* (1916) 17:448.

4. Wheeler JA. *Geometrodynamics*. New York: Academic (1962).

5. Misner CW, Thorne KS, Wheeler JA. San Francisco: Gravitation, Freeman (1973).

6. Morris MS, Thorne KS. Wormholes in spacetime and their use for interstellar travel: A tool for teaching general relativity. *Am J Phys* (1988) 56:395–412. doi:10.1119/1.15620

7. Hawking SW. Wormholes in spacetime. *Phys Rev D* (1988) 37:904–10. doi:10.1103/physrevd.37.904

8. Morris MS, Thorne KS, Yurtsever U. Wormholes, time machines, and the weak energy condition. *Phys Rev Lett* (1988) 61:1446–9. doi:10.1103/physrevlett.61.1446

9. Frolov VP, Novikov ID. Physical effects in wormholes and time machines. *Phys Rev D* (1990) 42:1057–65. doi:10.1103/physrevd.42.1057

10. Visser M, Kar S, Dadhich N. Traversable wormholes with arbitrarily small energy condition violations. *Phys Rev Lett* (2003) 90:201102. doi:10.1103/physrevlett.90.201102

11. Hochberg D, Visser M. Geometric structure of the generic static traversable wormhole throat. *Phys Rev D* (1997) 56:4745–55. doi:10.1103/physrevd.56.4745

12. Ida D, Hayward SA. How much negative energy does a wormhole need?. *Phys Lett A* (1999) 260:175–81. doi:10.1016/s0375-9601(99)00518-6

13. Fewster CJ, Roman TA. On wormholes with arbitrarily small quantities of exotic matter. *Phys Rev D* (2005) 72:044023. doi:10.1103/physrevd.72.044023

14. Kuhfittig PKF. More on wormholes supported by small amounts of exotic matter. *Phys Rev D* (2006) 73:084014. doi:10.1103/physrevd.73.084014

15. Rahaman F, Kalam M, Sarker M, Gayen K. A theoretical construction of wormhole supported by phantom energy. *Phys Lett B* (2006) 633:161–3. doi:10.1016/j.physletb.2005.11.080

16. Jamil M, Kuhfittig PKF, Rahaman F, Rakib SA. Wormholes supported by polytropic phantom energy. *Eur Phys J C* (2010) 67:513–20. doi:10.1140/epjc/s10052-010-1325-3

17. Teo E. Rotating traversable wormholes. *Phys Rev D* (1998) 58:024014. doi:10.1103/physrevd.58.024014

18. Kuhfittig PKF. Axially symmetric rotating traversable wormholes. *Phys Rev D* (2003) 67:064015. doi:10.1103/physrevd.67.064015

19. Hochberg D, Visser M. Dynamic wormholes, antitrapped surfaces, and energy conditions. *Phys Rev D* (1998) 58:044021. doi:10.1103/physrevd.58.044021

20. Hayward SA. Dynamic wormholes. *Int J Mod Phys D* (1999) 8:373–82. doi:10.1142/s0218271899000286

21. Lemos JPS, Lobo FSN, de Oliveira SQ. Morris-Thorne wormholes with a cosmological constant. *Phys Rev D* (2003) 68:064004. doi:10.1103/physrevd.68.064004

22. Rahaman F, Kalam M, Sarker M, Ghosh A, Raychaudhuri B. Wormhole with varying cosmological constant. *Gen Relativ Gravit* (2007) 39:145–51. doi:10.1007/s10714-006-0380-4

23. Wang D, Meng X-H. Traversable geometric dark energy wormholes constrained by astrophysical observations. *Eur Phys J C* (2016) 76:484. doi:10.1140/epjc/s10052-016-4321-4

24. Lobo FSN. Stability of phantom wormholes. *Phys Rev D* (2005) 71:124022. doi:10.1103/physrevd.71.124022

25. Banerjee A, Singh KN, Jasim M, Rahaman F. Conformally symmetric traversable wormholes in f(R, T) gravity. *Ann Phys* (2020) 422:168295. doi:10.1016/j.aop.2020.168295

26. Singh KN, Banerjee A, Rahaman F, Jasim MK. Conformally symmetric traversable wormholes in modified teleparallel gravity *Phys Rev D* (2020) 101:084012. doi:10.1103/PhysRevD.101.084012

27. Rahaman F, Sarkar S, Singh KN, Pant N. Generating functions of wormholes. *Mod Phys Lett A* (2019) 34:1950010. doi:10.1142/s021773231950010x

28. Banados M, Bautier K, Coussaert O, Henneaux M, Ortiz M. Anti–de Sitter–CFT correspondence in three-dimensional supergravity. *Phys Rev D* (1998) 58:085020. doi:10.1103/physrevd.58.085020

29. Cvetič M, Nojiri S, Odintsov SD. Cosmological anti–de Sitter space-times and time-dependent AdS/CFT correspondence. *Phys Rev D* (2004) 69:023513. doi:10.1103/physrevd.69.023513

30. Bao D, Chern SS, Shen Z. *An introduction to riemann-finsler geometry, graduate texts in mathematics*. New York: Springer (2000).

31. Rutz SF. A Finsler generalisation of Einstein's vacuum field equations. *Gen Relat Gravit* (1993) 25:1139–58. doi:10.1007/bf00763757

32. Vacaru S, Stavrinos P, Gaburov E, Gonta D. *Clifford and Riemann–Finsler structures in geometric mechanics and gravity*. Buchares: Geometry Balkan Press (2005).

33. Pfeifer C, Wohlfarth MNR. Finsler geometric extension of Einstein gravity. *Phys Rev D* (2012) 85:064009. doi:10.1103/physrevd.85.064009

34. Rahaman F, Paul N, Banerjee A, De SS, Ray S, Usmani AA. The Finslerian wormhole models. *Eur Phys J C* (2016) 76:246. doi:10.1140/epjc/s10052-016-4066-0

35. Girelli F, Liberati S, Sindoni L. Planck-scale modified dispersion relations and Finsler geometry. *Phys Rev D* (2007) 75:064015. doi:10.1103/physrevd.75.064015

36. Gibbons GW, Gomis J, Pope CN. General very special relativity is Finsler geometry. *Phys Rev D* (2007) 76:081701. doi:10.1103/physrevd.76.081701

37. Chang Z, Li X. Lorentz invariance violation and symmetry in Randers–Finsler spaces. *Phys Lett B* (2008) 663:103–6. doi:10.1016/j.physletb.2008.03.045

38. Kostelecky VA. Riemann–Finsler geometry and Lorentz-violating kinematics. *Phys Lett B* (2011) 701:137. doi:10.1016/j.physletb.2011.05.041

39. Kostelecky VA, Russell N, Tsoc R. Bipartite Riemann–Finsler geometry and Lorentz violation. *Phys Lett B* (2012) 716:470. doi:10.1016/j.physletb.2012.09.002

40. Kouretsis AP, Stathakopoulos M, Stavrinos PC. General very special relativity in Finsler cosmology. *Phys Rev D* (2009) 79:104011. doi:10.1103/physrevd.79.104011

41. Kouretsis AP, Stathakopoulos M, Stavrinos PC. Imperfect fluids, Lorentz violations, and Finsler cosmology. *Phys Rev D* (2010) 82:064035. doi:10.1103/physrevd.82.064035

42. Li X, Lin HN, Wang S, Chang Z. Anisotropic inflation in the Finsler spacetime. *Eur Phys J C* (2015) 75:260. doi:10.1140/epjc/s10052-015-3468-8

43. Minguzzi E. Raychaudhuri equation and singularity theorems in Finsler spacetimes. *Class Quan Grav* (2015) 32:185008. doi:10.1088/0264-9381/32/18/185008

44. Stavrinos PC, Alexiou M. Raychaudhuri equation in the Finsler–Randers space-time and generalized scalar-tensor theories. *Int J Geom Methods Mod Phys* (2018) 15:1850039. doi:10.1142/s0219887818500391

45. Aazami AB, Javaloyes MA. Penrose's singularity theorem in a Finsler spacetime. *Class Quan Grav* (2016) 33:025003. doi:10.1088/0264-9381/33/2/025003

46. Rahaman F, Paul N, De SS, Ray S, Jafry MAK. The Finslerian compact star model. *Eur Phys J C* (2015) 75:564. doi:10.1140/epjc/s10052-015-3797-7

47. Chowdhury SR. Hawking emission of charged particles from an electrically charged spherical black hole with scalar hair. *Eur Phys J C* (2019) 79:928. doi:10.1140/epjc/s10052-019-7452-6

48. Li X. Special finslerian generalization of the reissner-nordström spacetime. *Phys Rev D* (2018) 98:084030. doi:10.1103/physrevd.98.084030

49. Li X, Chang Z. Exact solution of vacuum field equation in Finsler spacetime. *Phys Rev D* (2014) 90:064049. doi:10.1103/physrevd.90.064049

50. Övgün A, Jusufi K, Sakallı İ. Exact traversable wormhole solution in bumblebee gravity. *Phys Rev D* (2019) 99:024042. doi:10.1103/physrevd.99.024042

51. Vacaru SI. *Springer Proc Math Stat* (2013) 439–43.

52. Övgün A, Sakalli I. A particular thin-shell wormhole. *Theor Math Phys* (2017) 190:120–9. doi:10.1134/s004057791701010x

53. Sakalli I, Ovgun A. Gravitinos tunneling from traversable Lorentzian wormholes. *Astrophys Space Sci* (2015) 359:32. doi:10.1007/s10509-015-2482-5

54. Sakalli I, Övgün A. Tunnelling of vector particles from Lorentzian wormholes in 3+1 dimensions. *Eur Phys J Plus* (2015) 130:110. doi:10.1140/epjp/i2015-15110-9

55. Jusufi K, Övgün A, Banerjee A, Sakallı İ. Gravitational lensing by wormholes supported by electromagnetic, scalar, and quantum effects. *Eur Phys J Plus* (2019) 134:428. doi:10.1140/epjp/i2019-12792-9

56. Lake MJ. Modelling cosmic springs with finsler and generalised finsler geometries. *Symmetry* (2022) 14:2166. doi:10.3390/sym14102166

57. Caxathodory C. *Variationsrechnung und partielle Differenialgleiehungenerster Ordnung*. Leipzig: Teubner Press (1935).

58. Bao D, Chern SS, Shen Z. *An introduction to riemann–finsler geometry*. New York: Springer (2000).

59. Akbar-Zadeh H. Sur les espaces de Finsler à courbures sectionnelles constantes. *Acad R Belg Bull Cl Sci* (1988) 74:281.

## Appendix A: Derivation of Einstein-Finsler field equation

Usually, the expression of the length for a curve in a Finslerian metric geometry is

$$S[\gamma] = \int d\tau \mathcal{F}(x(\tau), \dot{x}(\tau)). \tag{A1}$$

Lorentzian metric $g_{ab}$ defines the function $\mathcal{F}$ as $\mathcal{F}(x, \dot{x}) = |g_{ab}(x)\dot{x}^a\dot{x}^b|^{1/2}$ with $x$ and $\dot{x}$ signify respectively the position vector and tangent vector.

The Einstein-Finsler gravitational field equations are derived by the calculus of variations and in the framework of the tangent bundle of spacetime, i.e. can be derived from the action principle. Here the action (integral of Lagrangian density over spacetime) is defined as a union of the matter ($S_M$) and the Einstein-Hilbert ($S_{EH}$) action that couples gravity to matter and is given by

$$S = kS_{EH} + S_M.$$

In the Finsler space $(\mathbb{M}, \mathcal{F})$, the Einstein-Hilbert action could be reckoned over the sphere bundle $\Sigma$ as

$$S_{EH} = \int_\Sigma d^4\hat{x}\, d^3\theta \sqrt{g}\sqrt{h}\, \left(f_{ab}y^a y^b\right)\Big|_\Sigma. \tag{A2}$$

The action, i.e. the integral of Lagrangian density is varied with respect to $\mathcal{F}$ as all the quantities within the action are a function of $\mathcal{F}$ (i.e., on of $g$). Here $h_{ab}$ is the induced metric on $\Sigma$. The dynamics of $\mathcal{F}$ are equivalent to the Einstein equations.

Now,

$$\delta S_{EH} = \int d^4\hat{x}\, d^3\theta \sqrt{g}\sqrt{h}\left(\frac{1}{2}f_{ab}g^{ab}\delta g_{ab} + f_R\delta R_{ab} + \frac{1}{2}f_{ab}h^{ab}\delta h_{ab} - 2f_R R_{ab}\frac{\delta\mathcal{F}}{\mathcal{F}}\right)y^a y^b,$$

where $f_R = \partial f/\partial R$ and over the sphere bundle the function $f = f_{ab}y^a y^b$ [30]. Here, $\sqrt{g}$ and $R_{ab}$ do not depend on $\theta$. Now, the variation of $h^{ab}\delta h_{ab}$ is obtained as

$$h^{ab}\delta h_{ab} = \left(g^{ab} - y^a y^b\right)\delta g_{ab} - 6\frac{\delta\mathcal{F}}{\mathcal{F}}.$$

The relation between $\delta g_{ab}$ and $\frac{\delta\mathcal{F}}{\mathcal{F}}$ is

$$\delta g_{ab}(\hat{x}) = 2g_{ab}\frac{\delta\mathcal{F}}{\mathcal{F}}.$$

Using the above two equations, one can obtain finally

$$\delta S_{EH} = \int_\Sigma d^4\hat{x}\, d^3\theta\sqrt{g}\sqrt{h}(2fg_{ab} - 6f_{ab})y^a y^b\frac{\delta\mathcal{F}}{\mathcal{F}}.$$

In the Finslerian background the matter action for matter fields $\psi_i$ looks like ($L$ is the Lagrangian density of the matter fields)

$$S_M = \int_\Sigma d^4\hat{x}\, d^3\theta\sqrt{g}\sqrt{h}L(g, \psi_i).$$

Since $L$ and g are independent on $\theta$ over the fiber coordinates on the manifold $\mathbb{M}$, the integration of the system yields the standard matter action after dividing the volume of the three-sphere.

According to Pfeifer and Wohlfarth [33], in the Finsler background, the variation with respect to the Finsler function yields the Energy-Momentum tensor of p-form fields on Lorentzian metric spacetime as $T^{ab}$ as well as its trace $T = T^{ab}g_{ab} = 4L + 2g_{ab}\frac{\partial L}{\partial g_{ab}}$. Therefore, the variation with respect to the Finsler function gives

$$\delta S_M = \int_\Sigma d^4\hat{x}\, d^3\theta\sqrt{g}\sqrt{h}\left(12T_{ab} - 2Tg_{ab}\right)y^a y^b\frac{\delta\mathcal{F}}{\mathcal{F}}.$$

Next taking the variation with respect to $\mathcal{F}$ in the combined Einstein-Hilbert action with the matter yields

$$\begin{aligned}\delta S[\mathcal{F}, \psi_i] \quad &= k\delta S_E H + \delta S_M = \int_\Sigma d^4\hat{x}\, d^3\theta\sqrt{g}\sqrt{h}[k(2fg_{ab} - 6f_{ab}) \\ &\quad + (12T_{ab} - 2Tg_{ab})]y^a y^b\frac{\delta\mathcal{F}}{\mathcal{F}}.\end{aligned}$$

The structure of spacetime can be determined from the following equation,

$$[(3f + R)g_{ab} - 6f_{ab}]y^a y^b = -\frac{12T_{ab}}{k}y^a y^b.$$

Here we have considered the vanishing Cartan tensor and for that, the tensors in the bracket are $y$ independent.

The second derivative of the above with respect to fiber coordinates yields the Einstein-Finsler gravitational field equations as

$$R_{ab} - \frac{1}{2}S\, g_{ab} = \frac{1}{k}T_{ab}.$$

Here we set the coupling constant $k = \frac{c^4}{4\pi G}$.

To define the wormhole structure, we assume the Finsler structure is of the form

$$F^2 = B(r)y^t y^t - A(r)y^r y^r - r^2\bar{F}^2\left(\theta, \phi, y^\theta, y^\phi\right).$$

One can write the metric structure coefficient as

$$g_{\mu\nu} = \frac{\partial}{\partial y^\mu}\frac{\partial}{\partial y^\nu}\left(\frac{1}{2}F^2\right),$$

where $(g^{\mu\nu}) = (g_{\mu\nu})^{-1}$. Remember that each $g_{\mu\nu}$ is homogeneous of degree zero in $y$.

For a non-vanishing vector $y = y^\mu(\frac{\partial}{\partial x^\mu})|_p \in T_pM$, $\mathcal{F}$ persuades an inner product on $T_pM$ that is given by

$$g_y(u, v) = g_{\mu\nu}(x, y)u^\mu v^\nu, \tag{A3}$$

where $u = u^\mu(\frac{\partial}{\partial x^\mu})|_p$, $v = v^\mu(\frac{\partial}{\partial x^\mu})|_p \in T_pM\backslash\{0\}$.

The Finsler metric are given below

$$\begin{aligned}g_{\mu\nu} &= \mathrm{diag}\left(B, -A, -r^2\bar{g}_{ij}\right), \\ g^{\mu\nu} &= \mathrm{diag}\left(B^{-1}, -A^{-1}, -r^2\bar{g}^{ij}\right),\end{aligned}$$

where $\bar{g}^{ij}$ are derived from $\bar{F}^2$. In our study we have assumed $\lambda = \overline{Ric}$ which represents the Ricci scalar, derived from $\bar{F}^2$.